

Letter to the Editor
**Measurement of the electron temperature gradient
in a solar coronal hole**
C. David¹, A.H. Gabriel¹, F. Bely-Dubau², A. Fludra³, P. Lemaire¹, and K. Wilhelm⁴
¹ Institut d'Astrophysique Spatiale, Université Paris XI, F-91405 Orsay Cedex, France

² Observatoire de la Côte d'Azur, Lab. Cassini, F-06304 Nice Cedex 4, France

³ Rutherford Appleton Laboratory, Chilton, Didcot, Oxfordshire OX11 0QX, UK

⁴ Max-Planck-Institut für Aeronomie, D-37191 Katlenburg-Lindau, Germany

Received 8 April 1998 / Accepted 3 July 1998

Abstract. It has long been established that the high speed solar wind streams observed at 1 A.U. originate from the coronal hole regions of the Sun. Theoretical modelling of the acceleration mechanism depends critically on the value of the maximum of temperature existing close to the Sun. Measurements of the temperature in coronal holes prior to SOHO are unreliable. The very low luminosity leads to extreme observational difficulties, in particular due to light scattering in the instrument telescopes. Using the two SOHO spectrometers CDS and SUMER, electron temperatures have now been measured as a function of height above the limb in a polar coronal hole. Temperatures of around 0.8 MK are found close to the limb, rising to a maximum of less than 1 MK at $1.15 R_{\odot}$, then falling to around 0.4 MK at $1.3 R_{\odot}$. With these low temperatures, the classical Parker mechanism cannot alone explain the high wind velocities, which must therefore be due to the direct transfer of momentum from MHD waves to the ambient plasma.

Key words: coronal hole – fast solar wind

1. Introduction

It has been understood since the SKYLAB mission (Bohlin et al., 1975) that the high speed solar wind originates in solar holes. More recent data from ULYSSES (Woch et al., 1997) shows the importance of the polar coronal holes, particularly at times near the solar minimum, when a magnetic dipole dominates the configuration. The mechanism for accelerating the wind to the high values observed, of the order 800 km/s is not understood quantitatively. The Parker model is based upon a thermally driven wind (Parker 1958). To reach such high velocities, temperatures of the order 3 to 4 MK would be required near the base of the corona. However, other processes are available for acceleration of the wind, for example the direct transfer of momentum from MHD waves, with or without dissipation. This process results

from the decrease of momentum of the waves as they enter less dense regions, coupled with the need to conserve momentum of the total system consisting of the waves plus the local plasma. If this transfer predominates, it may not be necessary to invoke high coronal temperatures at the base of the corona.

In reality very little information was available on the temperature structure in coronal holes prior to the SOHO mission. Data from SKYLAB (Bohlin et al., 1975) is limited, due to the very low intensities in holes and the poor spectral resolution, leading to many line blends. SKYLAB was able to follow temperatures up to nearly 1 MK and no further and the interpretation of the data is quite uncertain (Habbal et al., 1993). The object of the present study is to exploit the superior performance of the instruments on SOHO in order to determine the temperature profile above a large polar coronal hole. If the observed gradient should prove to be positive with height, the possibility of temperatures of 3 to 4 MK at greater heights is not excluded. However, should the temperature fall with height from the 1 MK already known, then a thermally driven wind is excluded as a significant mechanism for the fast component.

Observations were carried out from SOHO on 21 May 1996 using the Joint Operations Programme JOP 002. We describe here a complete analysis of the data from the CDS(GIS) and SUMER spectrometers (Harrison et al., 1995, Wilhelm et al., 1995). A preliminary analysis has been reported previously (David et al., 1997a), which lacks the present complete treatment of the stray-light problem. Simultaneous observations were also carried out from UVCS and EIT instruments on SOHO, which can provide imaging and velocity data in the UV. Some further supporting sequences were performed on 21 November 1996, especially for clarifying the stray-light problem. In addition, some practice scans of the JOP 002 sequence, carried out on 15 May 1996 in a closed-field equatorial region provide important data, used for the inter-instrument calibration. Data from UVCS and EIT are not considered in this letter, but will be treated in a later publication. These instruments do not contribute directly to the measurement of electron temperatures, although their data

Send offprint requests to: gabriel@iaslab.ias.fr

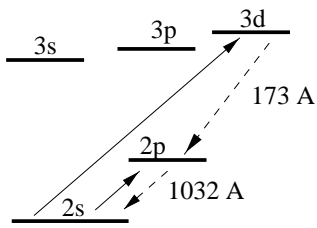


Fig. 1. Energy levels of O VI showing the lines used for electron temperature diagnostic

do help in the broader question of understanding the overall physics of the coronal hole and the acceleration process.

2. Method

In order to measure the electron temperature, we use the ratio of two lines from the same ion stage. This avoids the risk of non steady-state ionisation effect which could arise from the use of different ions. The choice of ion and transitions is based on the requirements to ensure that the ion exists over a wide temperature range and to have a high sensitivity to the electron temperature. These requirements are met optimally by the O VI ion, using the transitions 2s-2p at 1032 Å and 2p-3d 173 Å. The other possibility, using the 2s-3p transition at 150 Å, is not accessible to the CDS spectrometer. The two lines chosen are observed by two instruments, CDS and SUMER. Whilst this might be expected to pose difficulties for the calibration of the ratio, in practice we choose in this analysis to use the Sun itself as a calibration. This polar observing sequence was also performed in the closed field equatorial configuration. An assumed known temperature for this equatorial region of closed field then serves to calibrate the polar sequence. A possible systematic temperature uncertainty, of the order 10%, due to this approach is not of primary importance, and will have no effect on the measured difference between the equator and the poles, nor on the gradient of temperature with height. The alternative approach of using the known absolute intensity calibration of the two separate instruments would introduce an uncertainty greater than 30

Fig. 1 shows the energy levels responsible for the two transitions observed. Since the rate of excitation of the 2p level is much greater than that of the 3d level, we make the assumption that the ratio of the photon emission 2p-3d / 2s-2p is equal to the excitation rate ratio 2s-3d / 2s-2p. The values used for these collision rates are those calculated by Zhang et al. (1990). The O VI 2s-2p multiplet at 1032 Å and 1038 Å is also excited by photons, arising from the same transition in the more intense transition region. It can be shown (Noci et al., 1987) that whilst the collisional excitation process leads to a line ratio in this multiplet of 2.0, photon excitation alone would give a ratio of 4.0. We have used the departure of this measured ratio from 2.0 to correct for a photon excitation contamination of between 20% and 75%, retaining only the collisional component for the present temperature diagnostic.

Because of the very low emission from the corona in holes, and the need to avoid more intense emission from closed field regions along the line of sight, we choose to look at the corona above a large north polar hole. The slits of the SUMER and CDS/GIS spectrometers were co-aligned and made to scan a rectangular region from just inside the limb, out to 5 arcmin above the limb. The CDS/GIS channel is intrinsically astigmatic, so that the mean intensity along the length of the 4 arcmin slit is recorded without spatial resolution. In order to have a good spatial resolution in the radial direction it was therefore necessary to align the slits tangentially to the solar limb. This required that the SOHO spacecraft be rolled by 90 deg from its normal orientation throughout the period of the observation. This observing sequence, designated as JOP 002, has been negotiated with the other instruments of SOHO, to minimise the disturbance for the helioseismology measurements. It involves a period of not exceeding 16 hours in the rolled orientation. The region scanned starts 21 arcsec inside the limb and extends out to 5 arcmin beyond the limb. The total scanning sequence lasted 14 hours, giving progressively longer exposure times to the outer fainter positions.

For the coronal region beyond 1.05 R_{\odot} , the slit sizes used are 240×4 arcsec for CDS(GIS) and 300×1 arcsec for SUMER. To obtain the ratio for the same areas, the SUMER data was integrated over the inner 240 arcsec corresponding to the astigmatic CDS slit. Below this height, smaller area slits were used to avoid over-exposure of the detectors whilst on the disk. These lower height scans were used to establish the limb-crossing points, and thus the precise co-alignment of the two instruments. However, because of their low count-rates in the corona, their temperature data are not considered sufficiently reliable to include in the present results. The complex instrumental line profiles from the GIS detector, leads to a certain loss of spectral resolution. This was however sufficient to enable a good separation of the 173 Å from its two strong iron line neighbours, with an adequate estimation of the background count level between them. Another difficulty that can affect the the GIS detector is the possible contribution from “ghosts”. We are assured that the region of the 173 Å line should be free from this problem (Bromage and Del Zanna, private communication).

In the same wavelength range of O VI 173 Å, CDS provides many emission lines corresponding to different adjacent Fe ion stages. If we could assume steady-state ionisation equilibrium conditions, these lines could be used for another independent electron temperature diagnostic, based upon the theory of ionisation balance (Arnaud and Raymond, 1992). This assumption may not be valid in the case of a coronal hole, where the density is low and the wind flow is transporting the material across a temperature gradient. In the present case, where we have an independent measurement of electron temperature, we can however follow the intensity variation of these lines with altitude and try to understand the transient ionisation state of the plasma. This requires modelling of the density and flow velocity of the plasma. For the present we consider only a preliminary qualitative interpretation. The iron lines used for this analysis are listed in Table 1.

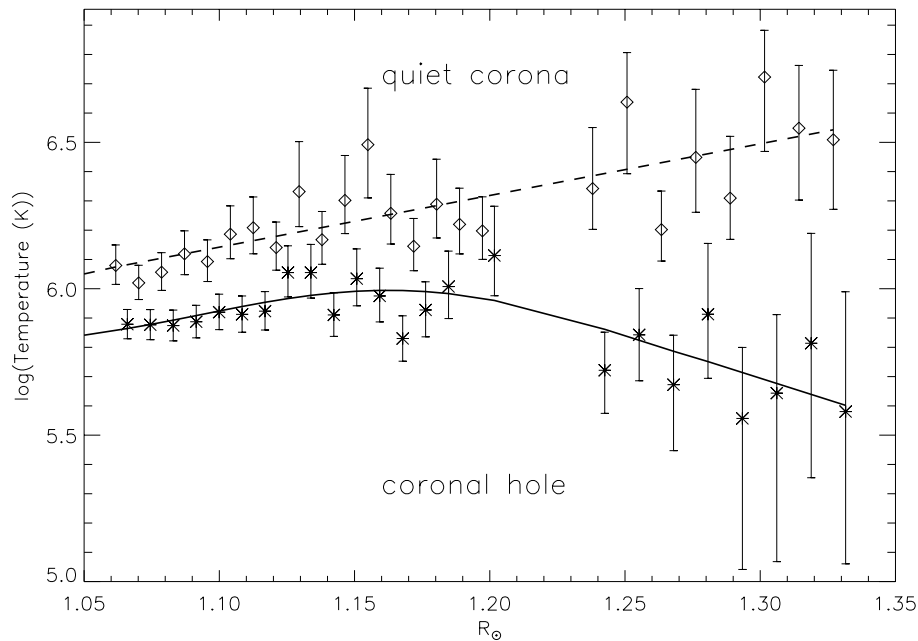


Fig. 2. Temperature gradient measurement in the quiet corona (equatorial west limb) and the north polar coronal hole

3. Correction for instrumental scattering

Although the telescope mirrors of both instruments are amongst the highest quality ever flown, their scattered light contribution is far from negligible, amounting in extreme cases to up to 80% of the measured signal. This situation is due to the fact that we are looking at quite faint regions, not far from much brighter and extended ones. It is therefore vital to make a reasonable correction for this component. The detailed method applied has been described elsewhere (David et al., 1997b). For SUMER, pre-launch measurement of the point-spread function is verified in flight by examining the apparent coronal extension of a purely disk emission in a C II line. The two measurements are made in the same wavelength region, which is also close in wavelength to the O VI lines used. For CDS, the pre-launch point-spread function measurements at 68 Å are related to the in-flight observations of O III disk emission at 703 Å using a theoretical wavelength variation relationship. The measured spectra near 173 Å are then corrected for stray light by an interpolation technique.

4. Electron temperature results

The measured temperatures are plotted in Fig. 2 as a function of radial distance, both for the polar hole observations of 21 May 1996 and the comparison scan at the equator, taken on 15 May 1996. The values plotted are derived from intensity ratios, corrected for instrumental scattering and after removal of the component due to photo-excitation. The calibration has been determined by adjusting the inner part of the closed field corona to a log T of 6.1, a figure consistent with a consensus of temperature values for the solar minimum quiet corona in closed-field regions. The indicated uncertainties are due in the lower corona to the estimated uncertainty in fitting instrumental profiles to the rather weak 173 Å line. At greater radial distances,

Table 1. Iron ion lines measured in the CDS/GIS range

Line	Wavelength(Å)
Fe VIII	168
Fe IX	171
Fe X	175
Fe XI	180
Fe XII	195
Fe XIII	203

uncertainties increase due to the increasing correction for instrumental scattering. Where this becomes a large fraction of the signal at the highest points, the combined uncertainties can lead to only upper limit error bars. The fitted curve for the coronal hole temperature shows that it is lower at all heights than that of the closed-field corona. The temperature rises to a maximum at around 1.15 R_{\odot} , which remains always below 1 MK, and then falls to around 0.4 MK at 1.3 R_{\odot} .

These measurements are in general agreement with other recent studies of coronal hole properties made by Wilhelm et al. (1998), using SUMER spectroscopic data. They derived electron temperatures using line ratios in the Magnesium IX ion. Compared with the present investigation, Magnesium IX has the advantage of a lower scattered light contribution, since it is weak on the solar disk. However, the nature of the atomic transitions employed, coupled with the calibration method used, are likely to give higher temperature errors of the order 20% to 30%. To within this precision, the values obtained of 0.8 MK falling to 0.3 MK at 1.6 R_{\odot} are consistent with the present results.

Mason et al. (1997) have made a multi-temperature differential emission measure analysis of a low-latitude coronal hole, viewed against the solar disk, using the CDS spectrometer on

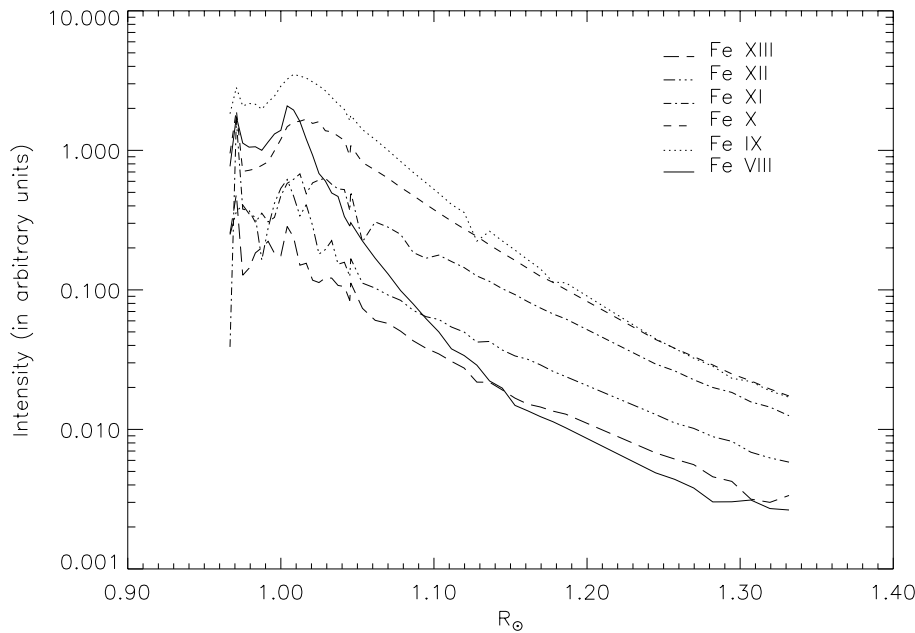


Fig. 3. Measurements of iron lines intensity in north polar coronal hole

SOHO. Their analysis is consistent with a maximum coronal temperature of below 1 MK.

We can readily reconcile the present results with previous observations made from SKYLAB. Single values of temperature derived from measurements on the disk will depend on parameters averaged over the first emission scale-height in the atmosphere. The present results are in this sense seen to be consistent with the measurements of 1 MK or less, reported from SKYLAB. Furthermore, a long-standing discrepancy between the UV temperature of holes and the radio brightness measurements (Lantos et al., 1992) may also be partially resolved by the present work. Radio brightness measurements in holes on the disk are typically only 0.3 or 0.5 MK. These values are lower than the modeling would predict, based upon the 1 MK previously believed to be the coronal hole temperature. This might now be more reasonable if the corona becomes optically thick to radio wavelengths at heights where the temperature is significantly lower. New multi-wavelength radio measurements of coronal hole temperatures may also help to resolve this question (Chiuderi-Drago, private communication).

Measurements made in a hole above the limb from the SXT on Yohkoh (Foley et al., 1997) have wide temperature error bars, due to the lower sensitivity of the broad-band X-ray channels. Even so, their results are rather high compared with the present measurements. This might be due to uncertainties in assuming the heavy element abundances in coronal hole regions.

It is of interest to try to compare the electron temperatures in the coronal hole/high-speed wind regions, over a very wide range of distances, using also Helios (Marsch et al., 1989) and Ulysses (Issautier et al., 1998) data. For the interplanetary data we consider the “core” electron temperature, ignoring the “halo” distribution. We find that the decrease in temperature around $1.3 R_{\odot}$ is too rapid to join smoothly with the interplanetary values of 0.1 MK at 0.5 A.U. or 0.05 MK at 2 A.U. This is not too

surprising, since the physics of the collision-dominated lower corona is distinctly different from that of the low-density interplanetary medium, dominated by collective plasma interactions.

5. Discussion

In the present work, we have assumed that the coronal hole plasma, seen above the limb, is isothermal along the line-of-sight. We should point out that several recent authors have tried to study the properties of solar plumes, which are observed in these regions (DeForrest et al. 1997, Wilhelm et al. 1998, Moses et al. 1997). Efforts to determine the difference between the plume and non-plume regions yield inconsistent results between the different authors. Here we assume that the difference in electron temperature between these regions is small (of the order 10% or less), justifying our adoption of a single averaged component in the holes.

In the equatorial scan, it can be seen that the temperature measured increases slowly with height. This result is consistent with measurements made from Yohkoh (Foley et al. 1995). For a closed field static structure, one might have expected an approximately constant temperature with height, due to the high thermal conductivity at these temperatures. The observed increase can be understood if, in these closed-field regions, we are looking at a succession of different field-lines with height, which impede a free conductive heat flow across the region.

The height variation of the different iron ion line intensities is shown in Fig. 3. These lines are formed primarily in the solar corona, so that instrumental scattering from the disk is not expected to be important, and has not been removed. Although these are given in arbitrary units, we can note that the ratios Fe IX/Fe VIII and Fe X/Fe IX both increase with height, showing an increasing ionization with time in the flowing plasma, in spite of the decreasing temperature. This may be evidence of a departure from ionization equilibrium due to the low density

and high flow-rate. On the other hand, the ratio of ions between Fe X and Fe XIII is fairly constant. A detailed modelling will be required in order to test this interpretation.

Observations using the SWICS instrument on Ulysses, during a south polar hole passage, have been used to derive “Freeze-in” temperatures from the balance of population of successive stages of ionisation of heavy ions, found in the solar wind (Ko et al. 1997). They deduce values of the order 1.5 MK at heights of $1.5 R_{\odot}$. These values are significantly outside of the present more direct measurements of coronal temperatures and pose questions regarding the assumptions implicit in interpreting freeze-in temperatures, concerning the recombination process or transport in the intervening interplanetary medium.

It is clear that the present observations preclude the existence of temperatures over 1 MK at any height near the centre of a coronal hole. Wind acceleration by temperature effects is therefore inadequate as an explanation of the high-speed wind and it becomes essential to look towards other effects, probably involving the momentum and the energy of Alfvén waves.

Acknowledgements. The SUMER project is financially supported by DLR, CNES, NASA and ESA-PRODEX (for the Swiss contribution). The CDS project acknowledges the support from many countries and Agencies (see Harrison et al., 1995). SOHO is a mission of international cooperation between ESA and NASA.

References

- Arnaud, M. and Raymond, J. 1992, *ApJ*, 398, 394–406
- Bohlin, J.D., Sheeley, N.R., Jr., and Tousey, R. 1975, in *Space Research*, Vol.15, ed. M.J. Rycroft (Berlin: Akademie-Verlag), 651
- David, C., Gabriel, A. and Bely-Dubau, F. 1997a. In: Proceedings of Fifth SOHO Workshop, “The Corona and Solar Wind Near Minimum Activity”, ESA SP-404, p.319
- David, C., Gabriel, A. and Bely-Dubau, F. 1997b. In: Proceedings of Fifth SOHO Workshop, “The Corona and Solar Wind Near Minimum Activity”, ESA SP-404, p.313
- DeForest, C.E., Hoeksema, J.T., Gurman, J.B., Thompson, B.J., Plunkett, S.P., Howard, R., Harrison, R.C. and Hassler, D.M. 1997, *Solar Phys.*, 175, 393–410
- Foley, C.R., Culhane, J.L., Acton, L.W. and Lemen, J.R. 1996. In: *Magnetodynamic Phenomena in Solar Atmosphere – Prototypes of Stellar Magnetic Activity*, éd. Y. Uchida et al., p. 419
- Foley, C.R., Culhane, J.L. and Acton, L.W. 1997, *ApJ*, 491, 933–938
- Habbal, S.R., Esser, R., and Arndt, M.B. 1993, *ApJ*, 413, 435–444
- Harrison, R. A et al. 1995, *Solar Phys.*, 162, 233–290
- Issautier, K., Meyer-Vernet, N., Moncuquet, M. and Hoang, S. 1998, *J. Geophys. Res.*, 103, 1969–1979
- Ko, Y.-K., Fisk, L.A., Geiss, J., Gloeckler, G. and Guhathakurta, M. 1997, *Solar Phys*, 171, 345–361
- Lantos, P., Alissandrakis, C.E. and Rigaud, D. 1992, *Solar Phys*, 137:225–256
- Marsch, E., Pilipp, W.G., Thieme, K.M. and Rosenbauer, H., 1989, *J. Geophys. Res.*, 94, 6893–6898
- Mason, H.E., Young, P.R., Pike, C.D., Harrison, R.A., Fludra, A., Bromage, B.J.I., and Del-Zanna, G. 1997, *Solar Phys*, 175, 571–599
- Moses, D. et al. 1997, *Solar Phys*, 170, 143–161
- Noci, G., Kohl, J.L., and Withbroe, G.L. 1987, *ApJ*, 315, 706–715
- Parker, E.N. 1958, *ApJ* 128, 664
- Wilhelm, K. et al. 1995, *Solar Phys.*, 162, 189–231
- Wilhelm, K., Marsch, E., Dwivedi, B.N., Hassler, D.M., Lemaire, P., Gabriel, A.H. and Huber, M.C.E. 1998, *ApJ*, 500, in press
- Woch, J., Axford, W.L., Mall, U., Wilken, B., Livi, S., Geiss, J., Gloeckler, G. and Forsyth, R.J. 1997, *Geophys. Res. Lett.*, 24, 22, p.2885
- Zhang, H.L., Sampson, D.H., and Fontes, C.J. 1990, *Atomic Data and Nuclear data tables*, 44, 31–77